FERMILAB-PUB-08-069-E
CDF Note 9290
DØ Note 5645

Combined CDF and DØ Upper Limits on Standard Model Higgs-Boson Production with up to 2.4 fb^{-1} of data

The TEVNPH Working Group*

for the CDF and DØ Collaborations

April 10, 2008

We combine results from CDF and DØ searches for a standard model Higgs boson (H) in $p\bar{p}$ collisions at the Fermilab Tevatron at $\sqrt{s} = 1.96$ TeV. With 1.0-2.4 fb^{-1} of data collected at CDF, and 1.1-2.3 fb^{-1} at DØ, the 95% C.L. upper limits on Higgs boson production are a factor of 3.7 (1.1) higher than the SM cross section for a Higgs boson mass of m_H =115 (160) GeV/c^2. Based on simulation, the median expected upper limit should be 3.3 (1.6). Standard Model branching ratios, calculated as functions of the Higgs boson mass, are assumed. Compared to the previous Higgs Tevatron combination, more data and new channels ($H \to \gamma\gamma$, and $H \to \tau\tau$ produced in several modes) have been added. Existing channels, such as both experiments' $ZH \to \nu\bar{\nu}b\bar{b}$ channels, have been reanalyzed to gain sensitivity. These results extend significantly the individual limits of each experiment.

Preliminary Results

* The Tevatron New-Phenomena and Higgs working group can be contacted at TEVNPHWG@fnal.gov. More information can be found at http://tevnphwg.fnal.gov/.

I. INTRODUCTION

The search for a mechanism for electroweak symmetry breaking, and in particular for a standard model (SM) Higgs boson boson has been a major goal of High Energy Physics for many years, and is a central part of Fermilab's Tevatron program. Both CDF and DØ have recently reported new searches for the SM Higgs boson that combined different production and decay modes [1, 2] that allow to gain sensitivity compared to the previous Tevatron combination presented in December 2007 [3]. In this note, we combine the most recent results of all such searches in $p\bar{p}$ collisions at $\sqrt{s} = 1.96$ TeV. The searches for a SM Higgs boson produced in association with vector bosons ($p\bar{p} \to WH \to \ell\nu b\bar{b}$, $p\bar{p} \to ZH \to \nu\bar{\nu}b\bar{b}/\ell^+\ell^- b\bar{b}$ or $p\bar{p} \to WH \to WW^+W^-$) or through gluon-gluon fusion ($p\bar{p} \to H \to W^+W^-$) or vector boson fusion (VBF), in data corresponding to integrated luminosities ranging from 1.0-2.4 fb^{-1} at CDF and 1.1-2.3 fb^{-1} at DØ. In this combination we add for the first time searches for Higgs bosons decaying to two photons or two tau leptons.

To simplify their combination, the searches are separated into twenty nine mutually exclusive final states (thirteen for CDF, sixteen for DØ, see Table I and II) referred to as "analyses" in this note. Selection procedures for each analysis are detailed in Refs. [5]-[13], and are briefly described below.

Compared to the results that we presented at the Moriond '08 conference [4], we adopt here a simpler approach in the treatment of the shape systematics uncertainties when deriving the final limits, treating them as Gaussian errors, as it is done for the other systematics uncertainties, instead of truncating them at $\pm 1\sigma$. This treatment is now consistent between the two limit setting methodologies described below. This change has essentially no effect on the expected limits and only affects the observed limits at low masses.

II. ACCEPTANCE, BACKGROUNDS AND LUMINOSITY

Event selections are similar for the corresponding CDF and DØ analyses. For the case of $WH \to \ell\nu b\bar{b}$, an isolated lepton (electron or muon) and two jets are required, with one or more b-tagged jet, i.e. identified as originating from a b-quark. Selected events must also display a significant imbalance in transverse momentum (referred to as missing transverse energy or $\not\!\!E_T$). Events with more than one isolated lepton are vetoed. For the DØ $WH \to \ell\nu b\bar{b}$ analyses, two non-overlapping b-tagged samples are defined, one being a single "tight" b-tag (ST) sample, and the other a double "loose" b-tag (DT) sample. The tight and loose b-tagging criteria are defined with respect to the mis-identification rate that the b-tagging algorithm yields for light quark or gluon jets ("mistag rate") typically $\leq 0.5\%$ or $\geq 1.5\%$, respectively. For the CDF $WH \to \ell\nu b\bar{b}$ analyses, an analysis based on a sample with two tight b-tags (TDT) is combined with an analysis based on a non-overlapping sample requiring one tight b-tag and one loose b-tag (LDT). For this combination additional channels have been added: a single b-tag channel (STC) with a dedicated neural network rejection of c-quark tagging , and three additional channels with similar b-tagging requirement, but with electrons detected in more forward directions than in the standard channels. In the $WH \to \ell\nu b\bar{b}$ analyses, both CDF and DØ use neural-network (NN) discriminants as the final variables for setting limits. The networks are optimized to discriminate signal from background at each value of the Higgs boson mass (the "test mass") under study.

For the $ZH \to \nu\bar{\nu}b\bar{b}$ analyses, the selection is similar to the WH selection, except all events with isolated leptons are vetoed and stronger multijet background suppression techniques are applied. The CDF analysis uses two non-overlapping samples of events (TDT and LDT as for WH) while DØ uses a sample of events having one tight b-tag jet and one loose b-tag jet. As there is a sizable fraction of $WH \to \ell\nu b\bar{b}$ signal in which the lepton is undetected, that is selected in the $ZH \to \nu\bar{\nu}b\bar{b}$ samples, the DØ analysis includes this fraction as a separate search, referred to as $WH \to \not\ell\nu b\bar{b}$. CDF includes it as this fraction is included as part of the acceptance of the $ZH \to \nu\bar{\nu}b\bar{b}$ search. Compared to the previous combination, CDF is now also using a neural-network discriminant as final variable, while DØ has doubled the analyzed statistics and uses now boosted decision trees instead of neural networks as advanced analysis technique.

The $ZH \to \ell^+\ell^- b\bar{b}$ analyses require two isolated leptons and at least two jets. They use non-overlapping samples of events with one tight b-tag and two loose b-tags. For the DØ analysis a neural-network discriminant is the final variable for setting limits, while CDF uses the output of a 2-dimensional neural-network. These analyses have not been updated compared to the previous combination.

For the $H \to W^+W^-$ analyses, a large $\not\!\!E_T$ and two opposite-signed, isolated leptons (any combination of electrons or muons) are selected, defining three final states (e^+e^-, $e^\pm\mu^\mp$, and $\mu^+\mu^-$) for DØ. CDF separates the $H \to W^+W^-$ events in two non-overlapping samples, one having a low signal/bacgkround (S/B) ratio, the other having a higher one. The presence of neutrinos in the final state prevents reconstruction of the Higgs boson mass. The final discriminants are neural-network outputs including likelihoods constructed from matrix-element probabilities as input to the neural network, for both CDF and DØ. All analyses in this channel have been updated with more data and analysis improvements.

The CDF experiment contributes also a new analysis searching for Higgs bosons decaying to a tau lepton pair, in three separate production channel with 2 fb^{-1} of data: direct $p\bar{p} \to H$ production, associated WH or ZH production, or vector boson production with H and forward jets in the final state. In this analysis, the final variable for setting limits is a combination of several neural-network discriminants.

The DØ experiment contributes three $WH \to WW^+W^-$ analyses, where the associated W boson and the W boson from the Higgs boson decay which has the same charge are required to decay leptonically, thereby defining three like-sign dilepton final states ($e^\pm e^\pm$, $e^\pm\mu^\pm$, and $\mu^\pm\mu^\pm$) containing all decays of the third W boson. In this analysis, which has not been updated for this combination, the final variable is a likelihood discriminant formed from several topological variables. DØ also contributes a new analysis searching for direct Higgs boson production decaying to a photon pair in 2.3 fb^{-1} of data. In this analysis, the final variable is the invariant mass of the two photons system.

All Higgs boson signals are simulated using PYTHIA [17], and CTEQ5L or CTEQ6L [18] leading-order (LO) parton distribution functions. The signal cross sections are normalized to next-to-next-to-leading order (NNLO) calculations [19, 20], and branching ratios from HDECAY [21]. For both CDF and DØ, events from multijet (instrumental) backgrounds ("QCD production") are measured in data with different methods, in orthogonal samples. For CDF, backgrounds from other SM processes were generated using PYTHIA, ALPGEN [22], MC@NLO [23] and HERWIG [24] programs. For DØ, these backgrounds were generated using PYTHIA, ALPGEN, and COMPHEP [25], with PYTHIA providing parton-showering and hadronization for all the generators. Background processes were normalized using either experimental data or next-to-leading order calculations from MCFM [26].

Integrated luminosities, and references to the collaborations' public documentation for each analysis are given in Table I for CDF and in Table II for DØ. The tables include the ranges of Higgs boson mass (m_H) over which the searches were performed.

TABLE I: Luminosity, explored mass range and references for the CDF analyses. ℓ stands for either e or μ.

	$WH \to \ell\nu b\bar{b}$ 2 (TDT,LDT,STC)	$ZH \to \nu\bar{\nu}b\bar{b}$ TDT,LDT	$ZH \to \ell^+\ell^-b\bar{b}$ ST,DT	$H \to W^+W^-$ low,high S/B	$H + X \to \tau^+\tau^- + 2$ jets H+VBF+WH+ZH
Luminosity (fb^{-1})	1.9	1.7	1.0	2.4	2.0
m_H range (GeV/c^2)	110-150	100-150	110-150	110-200	110-150
Reference	[5]	[6]	[7]	[8]	[9]

TABLE II: Luminosity, explored mass range and references for the DØ analyses. ℓ stands for either e or μ.

	$WH \to \ell\nu b\bar{b}$ 2 (ST,DT)	$ZH \to \nu\bar{\nu}b\bar{b}$ DT	$ZH \to \ell^+\ell^-b\bar{b}$ 2 (ST,DT)	$H \to W^+W^-$ $\to \ell^\pm\nu\ell^\mp\nu$	$WH \to WW^+W^-$ $\to \ell^\pm\nu\ell^\pm\nu$	$H \to \gamma\gamma$
Luminosity (fb^{-1})	1.7	2.1	1.1	2.3	1.1	2.3
m_H range (GeV/c^2)	105-145	105-145	105-145	110-200	120-200	105-145
Reference	[10]	[11]	[12]	[13],[14]	[15]	[16]

III. COMBINING CHANNELS

To gain confidence that the final result does not depend on the details of the statistical formulation, we performed several types of combinations, using the Bayesian and Modified Frequentist approaches, which give similar results (within 10%). Both methods rely on distributions in the final discriminants, and not just on their single integrated values. Systematic uncertainties enter as uncertainties on the expected number of signal and background events, as well as on the distribution of the discriminants in each analysis ("shape uncertainties"). Both methods use likelihood calculations based on Poisson probabilities.

A. Bayesian Method

Because there is no experimental information on the production cross section for the Higgs boson, in the Bayesian technique [1] we assign a flat prior for the total number of selected Higgs events. For a given Higgs boson mass, the combined likelihood is a product of likelihoods for the individual channels, each of which is a product over histogram bins:

$$\mathcal{L}(R,\vec{s},\vec{b}|\vec{n},\vec{\theta})\times\pi(\vec{\theta}) = \prod_{i=1}^{N_C}\prod_{j=1}^{Nbins}\mu_{ij}^{n_{ij}}e^{-\mu_{ij}}/n_{ij}!\times\prod_{k=1}^{n_{np}}e^{-\theta_k^2/2} \tag{1}$$

where the first product is over the number of channels (N_C), and the second product is over histogram bins containing n_{ij} events, binned in ranges of the final discriminants used for individual analyses, such as the dijet mass, neural-network outputs, or matrix-element likelihoods. The parameters that contribute to the expected bin contents are $\mu_{ij} = R\times s_{ij}(\vec{\theta}) + b_{ij}(\vec{\theta})$ for the channel i and the histogram bin j, where s_{ij} and b_{ij} represent the expected background and signal in the bin, and R is a scaling factor applied to the signal to test the sensitivity level of the experiment. Truncated Gaussian priors are used for each of the nuisance parameters θ_k, which define the sensitivity of the predicted signal and background estimates to systematic uncertainties. These can take the form of uncertainties on overall rates, as well as the shapes of the distributions used for combination. These systematic uncertainties can be far larger than the expected SM signal, and are therefore important in the calculation of limits. The truncation is applied so that no prediction of any signal or background in any bin is negative. The posterior density function is then integrated over all parameters (including correlations) except for R, and a 95% credibility level upper limit on R is estimated by calculating the value of R that corresponds to 95% of the area of the resulting distribution.

B. Modified Frequentist Method

The Modified Frequentist technique relies on the CL_s method, using a log-likelihood ratio (LLR) as test statistic [2]:

$$LLR = -2\ln\frac{p(\text{data}|H_1)}{p(\text{data}|H_0)}, \tag{2}$$

where H_1 denotes the test hypothesis, which admits the presence of SM backgrounds and a Higgs boson signal, while H_0 is the null hypothesis, for only SM backgrounds. The probabilities p are computed using the best-fit values of the nuisance parameters for each event, separately for each of the two hypotheses, and include the Poisson probabilities of observing the data multiplied by Gaussian constraints for the values of the nuisance parameters. This technique extends the LEP procedure [27] which does not involve a fit, in order to yield better sensitivity when expected signals are small and systematic uncertainties on backgrounds are large.

The CL_s technique involves computing two p-values, CL_{s+b} and CL_b. The latter is defined by

$$1 - CL_b = p(LLR \le LLR_{\text{obs}}|H_0), \tag{3}$$

where $LLR_{\rm obs}$ is the value of the test statistic computed for the data. $1 - CL_b$ is the probability of observing a signal-plus-background-like outcome without the presence of signal, i.e. the probability that an upward fluctuation of the background provides a signal-plus-background-like response as observed in data. The other p-value is defined by

$$CL_{s+b} = p(LLR \geq LLR_{\rm obs}|H_1), \tag{4}$$

and this corresponds to the probability of a downward fluctuation of the sum of signal and background in the data. A small value of CL_{s+b} reflects inconsistency with H_1. It is also possible to have a downward fluctuation in data even in the absence of any signal, and a small value of CL_{s+b} is possible even if the expected signal is so small that it cannot be tested with the experiment. To minimize the possibility of excluding a signal to which there is insufficient sensitivity (an outcome expected 5% of the time at the 95% C.L., for full coverage), we use the quantity $CL_s = CL_{s+b}/CL_b$. If $CL_s < 0.05$ for a particular choice of H_1, that hypothesis is deemed excluded at the 95% C.L.

Systematic uncertainties are included by fluctuating the predictions for signal and background rates in each bin of each histogram in a correlated way when generating the pseudoexperiments used to compute CL_{s+b} and CL_b.

C. Systematic Uncertainties

Systematic uncertainties differ between experiments and analyses, and they affect the rates and shapes of the predicted signal and background in correlated ways. The combined results incorporate the sensitivity of predictions to values of nuisance parameters, and correlations are included, between rates and shapes, between signals and backgrounds, and between channels within experiments and between experiments. More on these issues can be found in the individual analysis notes [5]-[16]. Here we consider only the largest contributions and correlations between and within the two experiments.

1. Correlated Systematics between CDF and DØ

The uncertainty on the measurement of the integrated luminosity is 6% (CDF) and 6.1% (DØ). Of this value, 4% arises from the uncertainty on the inelastic $p\bar{p}$ scattering cross section, which is correlated between CDF and DØ. The uncertainty on the production rates for the signal, for top-quark processes ($t\bar{t}$ and single top) and for electroweak processes (WW, WZ, and ZZ) are taken as correlated between the two experiments. As the methods of measuring the multijet ("QCD") backgrounds differ between CDF and DØ, there is no correlation assumed between these rates. Similarly, the large uncertainties on the background rates for W+heavy flavor (HF) and Z+heavy flavor are considered at this time to be uncorrelated, as both CDF and DØ estimate these rates using data control samples, but employ different techniques. The calibrations of fake leptons, unvetoed $\gamma \to e^+e^-$ conversions, b-tag efficiencies and mistag rates are performed by each collaboration using independent data samples and methods, hence are considered uncorrelated.

2. Correlated Systematic Uncertainties for CDF

The dominant systematic uncertainties for the CDF analyses are shown in Tables III,VI,VII, IX, XI. Each source induces a correlated uncertainty across all CDF channels sensitive to that source. For $H \to b\bar{b}$, the largest uncertainties on signal arise from a scale factor for b-tagging (5.3-16%), jet energy scale (1-20%) and MC modeling (2-10%). The shape dependence of the jet energy scale, b-tagging and uncertainties on gluon radiation ("ISR" and "FSR") are taken into account for some analyses (see tables). For $H \to W^+W^-$, the largest uncertainty comes from MC modeling (5%). For simulated backgrounds, the uncertainties on the expected rates range from 11-40% (depending on background). The backgrounds with the largest systematic uncertainties are in general quite small. Such uncertainties are constrained by fits to the nuisance parameters, and they do not affect the result significantly. Because the largest background contributions are measured using data, these uncertainties are treated as uncorrelated for the $H \to b\bar{b}$ channels. For the $H \to W^+W^-$ channel, the uncertainty on luminosity is taken to be correlated between signal

TABLE III: Systematic uncertainties on the signal contributions for CDF's loose double tag (LDT) channel and tight double-tag (TDT) channel. Systematic uncertainties are listed by name, see the original references for a detailed explanation of their meaning and on how they are derived. Systematic uncertainties for WH shown in this table are obtained for $m_H = 115$ GeV/c^2. Uncertainties are relative, in percent and are symmetric unless otherwise indicated.

CDF: Loose Double Tag (LDT) WH Analysis

Contribution	W+HF	Mistags	Top	Diboson	Non-W	WH
Luminosity ($\sigma_{\rm inel}(p\bar{p})$)	0	0	4	4	0	4
Luminosity Monitor	0	0	5	5	0	5
Lepton ID	0	0	2	2	0	2
Jet Energy Scale	0	0	0	0	0	3
Mistag Rate	0	8	0	0	0	0
B-Tag Efficiency	0	0	0	0	0	8
$t\bar{t}$ Cross Section	0	0	15	0	0	0
Diboson Rate	0	0	0	10	0	0
NNLO Cross Section	0	0	0	0	0	1
HF Fraction in W+jets	42	0	0	0	0	0
ISR+FSR+PDF	0	0	0	0	0	5
QCD Rate	0	0	0	0	18	0

CDF: Tight Double Tag (TDT) WH Analysis

Contribution	W+HF	Mistags	Top	Diboson	Non-W	WH
Luminosity ($\sigma_{\rm inel}(p\bar{p})$)	0	0	4	4	0	4
Luminosity Monitor	0	0	5	5	0	5
Lepton ID	0	0	2	2	0	2
Jet Energy Scale	0	0	0	0	0	3
Mistag Rate	0	9	0	0	0	0
B-Tag Efficiency	0	0	0	0	0	9
$t\bar{t}$ Cross Section	0	0	15	0	0	0
Diboson Rate	0	0	0	10	0	0
NNLO Cross Section	0	0	0	0	0	1
HF Fraction in W+jets	42	0	0	0	0	0
ISR+FSR+PDF	0	0	0	0	0	6
QCD Rate	0	0	0	0	18	0

and background. The differences in the resulting limits whether treating the remaining uncertainties as correlated or uncorrelated, is 5%.

3. Correlated Systematic Uncertainties for DØ

The dominant systematic uncertainties for DØ analyses are shown in Tables IV,V,VIII,X,XII, XIII. Each source induces a correlated uncertainty across all DØ channels sensitive to that source. The $H \to b\bar{b}$ analyses have an uncertainty on the b-tagging rate of 3-10% per tagged jet, and also an uncertainty on the jet energy and acceptance of 6-9% (jet identification or jet ID, energy scale, and jet resolution). The shape dependence of the uncertainty on $W+$ jet modeling is taken into account in the limit setting, and has a small effect ($\sim 5\%$) on the final result. For the $H \to W^+W^-$ and $WH \to WW^+W^-$, the largest uncertainties are associated with lepton measurement and acceptance. These values range from 2-11% depending on the final state. The largest contributing factor to all analyses is the uncertainty on cross sections for simulated background, and is 6-18%. All systematic uncertainties arising from the same source are taken to be correlated between the different backgrounds and between signal and background.

TABLE IV: Systematic uncertainties on the signal contributions for DØ's $WH \to \ell\nu b\bar{b}$ single (ST) and double tag (DT) channel. Systematic uncertainties are listed by name, see the original references for a detailed explanation of their meaning and on how they are derived. Systematic uncertainties for WH shown in this table are obtained for $m_H = 115$ GeV/c^2. Uncertainties are relative, in percent and are symmetric unless otherwise indicated.

DØ: Single Tag (ST) WH Analysis

Contribution	WZ/WW	Wbb/Wcc	Wjj/Wcj	$t\bar{t}$	single top	QCD	WH
Luminosity	6.1	6.1	6.1	6.1	6.1	0	6.1
Trigger eff.	3	3	3	3	3	0	3
Primary Vertex/misc.	4	4	4	4	4	0	4
EM ID/Reco eff./resol.	5	5	5	5	5	0	5
Muon ID/Reco eff./resol.	7	7	7	7	7	0	7
Jet ID/Reco eff.	3	3	3	3	3	0	3
Jet multiplicity/frag.	5	5	5	5	5	0	5
Jet Energy Scale	3	4	3	4	2	0	3
Jet taggability	3	3	3	3	3	0	3
NN b-tagger Scale Factor	3	3	15	3	3	0	3
Cross Section	6	9	9	16	16	0	6
Heavy-Flavor K-factor	0	20	20	0	0	0	0
Instrumental-WH-1	0	0	0	0	0	19	0

DØ: Double Tag (DT) WH Analysis

Contribution	WZ/WW	Wbb/Wcc	Wjj/Wcj	$t\bar{t}$	single top	QCD	WH
Luminosity	6.1	6.1	6.1	6.1	6.1	0	6.1
Trigger eff.	3	3	3	3	3	0	3
Primary Vertex/misc.	4	4	4	4	4	0	4
EM ID/Reco eff./resol.	5	5	5	5	5	0	5
Muon ID/Reco eff./resol.	7	7	7	7	7	0	7
Jet ID/Reco eff.	3	3	3	3	3	0	3
Jet multiplicity/frag.	5	5	5	5	5	0	5
Jet Energy Scale	3	4	3	4	2	0	3
Jet taggability	3	3	3	3	3	0	3
NN b-tagger Scale Factor	6	6	25	6	6	0	6
Cross Section	6	9	9	16	16	0	6
Heavy-Flavor K-factor	0	20	2	0	0	0	0
Instrumental-WH-2	0	0	0	0	0	31	0

TABLE V: Systematic uncertainties on the contributions for DØ's $ZH \to \nu\nu b\bar{b}$ double-tag (DT) channel. Systematic uncertainties are listed by name, see the original references for a detailed explanation of their meaning and on how they are derived. Systematic uncertainties for ZH, WH shown in this table are obtained for $m_H = 115$ GeV/c^2. Uncertainties are relative, in percent and are symmetric unless otherwise indicated.

DØ: Double Tag (DT) $ZH \to \nu\nu b\bar{b}$ Analysis

Contribution	WZ/ZZ	Z+jets	W+jets	$t\bar{t}$	ZH,WH
Luminosity	6.1	6.1	6.1	6.1	6.1
Trigger eff.	5	5	5	5	5
Jet Energy Scale	3	3	3	3	2
Jet ID/resolution.	2	2	2	2	2
B-tagging/taggability	6	6	6	6	6
Cross Section	6	15	15	18	6
Heavy Flavour K-factor	-	50	50	-	-

TABLE VI: Systematic uncertainties for CDF's $ZH \to \nu\bar{\nu}b\bar{b}$ loose double tag (LDT) channel and tight double-tag (TDT) channel. Systematic uncertainties are listed by name, see the original references for a detailed explanation of their meaning and on how they are derived. Systematic uncertainties for ZH and WH shown in this table are obtained for $m_H = 120$ GeV/c^2. Uncertainties are relative, in percent and are symmetric unless otherwise indicated.

CDF: Loose Double Tag (LDT) $ZH \to \nu\nu b\bar{b}$ Analysis

Contribution	Mistag	QCD	Single top	$t\bar{t}$	WW	WZ	ZZ	$W \to \ell\nu$	$Z \to \ell\ell/\nu\nu$	ZH	WH
Luminosity ($\sigma_{\rm inel}(p\bar{p})$)	0	0	4	4	4	4	4	4	4	4	4
Luminosity Monitor	0	0	5	5	5	5	5	5	5	5	5
Trigger (shape dep.)	0	0	4	3	4	4	4	4	4	4	3
Lepton Veto	0	0	2	2	2	2	2	2	2	2	2
Jet Energy Scale (shape dep.)	0	0	$^{+4}_{-7}$	$^{-11}_{-4}$	$^{+4}_{-8}$	$^{+4}_{-8}$	$^{+9}_{-9}$	$^{+6}_{-13}$	$^{+13}_{-9}$	$^{+3}_{-6}$	$^{-6}_{-2}$
Mistag Rate (shape dep.)	29	0	0	0	0	0	0	0	0	0	0
B-Tag Efficiency	0	0	9.2	9.2	9.2	9.2	9.2	9.2	9.2	9.2	9.2
$\sigma(p\bar{p} \to Z + HF)$	0	0	0	0	0	0	0	0	40	0	0
$\sigma(p\bar{p} \to W + HF)$	0	0	0	0	0	0	0	40	0	0	0
Diboson Cross Section	0	0	0	0	11.5	11.5	11.5	0	0	0	0
$t\bar{t}$ Cross Section	0	0	0	10	0	0	0	0	0	0	0
Single Top Cross Section	0	0	11.5	0	0	0	0	0	0	0	0
ISR	0	0	0	0	0	0	0	0	0	$^{+5.0}_{-1.7}$	$^{+4.9}_{+0.4}$
FSR	0	0	0	0	0	0	0	0	0	$^{+0.4}_{+4.9}$	$^{+2.5}_{+5.2}$
PDF Uncertainty	0	0	2	2	2	2	2	2	2	2	2
QCD Rate (shape dep.)	0	50	0	0	0	0	0	0	0	0	0

CDF: Tight Double Tag (TDT) $ZH \to \nu\nu b\bar{b}$ Analysis

Contribution	Mistag	QCD	Single top	$t\bar{t}$	WW	WZ	ZZ	$W \to \ell\nu$	$Z \to \ell\ell/\nu\nu$	ZH	WH
Luminosity ($\sigma_{\rm inel}(p\bar{p})$)	0	0	4	4	4	4	4	4	4	4	4
Luminosity Monitor	0	0	5	5	5	5	5	5	5	5	5
Trigger	0	0	4	3	5	5	4	4	4	4	4
Lepton Veto	0	0	2	2	2	2	2	2	2	0	0
Jet Energy Scale (shape dep.)	0	0	$^{-5}_{-7}$	$^{-9}_{-3}$	$^{+7}_{-8}$	$^{+7}_{-8}$	$^{+8}_{-7}$	$^{+6}_{-12}$	$^{+10}_{-6}$	$^{+2}_{-6}$	$^{+3}_{+7}$
Mistag Rate-2 (shape dep.)	23	0	0	0	0	0	0	0	0	0	0
B-Tag Efficiency	0	8.6	8.6	8.6	8.6	8.6	8.6	8.6	8.6	8.6	8.6
$\sigma(p\bar{p} \to Z + HF)$	0	0	0	0	0	0	0	0	40	0	0
$\sigma(p\bar{p} \to W + HF)$	0	0	0	0	0	0	0	40	0	0	0
Diboson Cross Section	0	0	0	0	11.5	11.5	11.5	0	0	0	0
$t\bar{t}$ Cross Section	0	0	0	10	0	0	0	0	0	0	0
Single Top Cross Section	0	0	11.5	0	0	0	0	0	0	0	0
ISR	0	0	0	0	0	0	0	0	0	$^{+5.0}_{-1.7}$	$^{+4.9}_{+0.4}$
FSR	0	0	0	0	0	0	0	0	0	$^{+0.4}_{+4.9}$	$^{+2.5}_{+5.2}$
PDF	0	0	2	2	2	2	2	2	2	2	2
QCD Rate (shape dep.)	0	50	0	0	0	0	0	0	0	0	0

TABLE VII: Systematic uncertainties on the contributions for CDF's $ZH \to \ell^+\ell^- b\bar{b}$ single-tag (ST) channel. Systematic uncertainties are listed by name, see the original references for a detailed explanation of their meaning and on how they are derived. Systematic uncertainties for ZH shown in this table are obtained for $m_H = 115$ GeV/c^2. Uncertainties are relative, in percent and are symmetric unless otherwise indicated.

CDF: Single Tag (ST) $ZH \to \ell\ell b\bar{b}$ Analysis

Contribution	Fakes	Top	WZ	ZZ	$Z + bb$	$Z + c\bar{c}$	Z+mistag	ZH
Luminosity ($\sigma_{\rm inel}(p\bar{p})$)	0	4	4	4	4	4	0	4
Luminosity Monitor	0	5	5	5	5	5	0	5
Lepton ID	0	1	1	1	1	1	0	1
Fake Leptons	50	0	0	0	0	0	0	0
Jet Energy Scale (shape dep.)	0	$^{+1.3}_{-2.6}$	$^{+1.9}_{-4.4}$	$^{+4.1}_{-4.4}$	$^{+12.8}_{-12.4}$	$^{+0.11.3}_{-9.8}$	0	$^{+2.3}_{-2.4}$
Mistag Rate	0	0	0	0	0	0	13	0
B-Tag Efficiency	0	8	8	8	8	16	0	8
$t\bar{t}$ Cross Section	0	20	0	0	0	0	0	0
Diboson Cross Section	0	0	20	0	0	0	0	0
$\sigma(p\bar{p} \to Z + HF)$	0	0	0	0	40	40	0	0
ISR (shape dep.)	0	0	0	0	0	0	0	$^{+1.1}_{+0.4}$
FSR (shape dep.)	0	0	0	0	0	0	0	$^{-0.7}_{-1.4}$

CDF: Double Tag (DT) $ZH \to \ell\ell b\bar{b}$ Analysis

Contribution	Fakes	Top	WZ	ZZ	$Z + bb$	$Z + c\bar{c}$	Z+mistag	ZH
Luminosity ($\sigma_{\rm inel}(p\bar{p})$)	0	4	4	4	4	4	0	4
Luminosity Monitor	0	5	5	5	5	5	0	5
Lepton ID	0	1	1	1	1	1	0	1
Fake Leptons	50	0	0	0	0	0	0	0
Jet Energy Scale (shape dep.)	0	$^{+0.1}_{-0.1}$	0	$^{+0.5}_{-3.0}$	$^{+3.1}_{-7.8}$	$^{+8.7}_{-0}$	0	$^{+0.3}_{-1.2}$
Mistag Rate	0	0	0	0	0	0	24	0
B-Tag Efficiency	0	16	16	16	16	32	0	16
$t\bar{t}$ Cross Section	0	20	0	0	0	0	0	0
Diboson Cross Section	0	0	20	0	0	0	0	0
$\sigma(p\bar{p} \to Z + HF)$	0	0	0	0	40	40	0	0
ISR (shape dep.)	0	0	0	0	0	0	0	$^{+4.6}_{+0.6}$
FSR (shape dep.)	0	0	0	0	0	0	0	$^{+5.3}_{+3.7}$

TABLE VIII: Systematic uncertainties on the contributions for DØ's $ZH \to \ell^+\ell^- b\bar{b}$ single-tag (ST) channel. Systematic uncertainties are listed by name, see the original references for a detailed explanation of their meaning and on how they are derived. Systematic uncertainties for ZH shown in this table are obtained for $m_H = 115$ GeV/c^2. Uncertainties are relative, in percent and are symmetric unless otherwise indicated.

DØ: Single Tag (ST) $ZH \to \ell\ell b\bar{b}$ Analysis

Contribution	WZ/ZZ	Zbb/Zcc	Zjj	$t\bar{t}$	QCD	ZH
Luminosity	6.1	6.1	6.1	6.1	0	6.1
EM ID/Reco eff.	4	4	4	4	0	4
Muon ID/Reco eff.	4	4	4	4	0	4
Jet ID/Reco eff.	2	1.5	2	1.5	0	1.5
Jet Energy Scale (shape dep.)	4	8	11	2	0	2
B-tagging/taggability	7	6	9	3	0	3
Cross Section	7	0	0	18	0	6
Heavy-Flavor K-factor	0	30	15	0	0	0
Instrumental-ZH-1	0	0	0	0	50	0

DØ: Double Tag (DT) $ZH \to \ell\ell b\bar{b}$ Analysis

Contribution	WZ/ZZ	Zbb/Zcc	Zjj	$t\bar{t}$	QCD	ZH
Luminosity	6.1	6.1	6.1	6.1	0	6.1
EM ID/Reco eff.	4	4	4	4	0	4
Muon ID/Reco eff.	4	4	4	4	0	4
Jet ID/Reco eff.	2	1.5	2	1.5	0	1.5
Jet Energy Scale (shape dep.)	4	8	11	2	0	2
B-tagging/taggability	8	8	9	7	0	7
Cross Section	7	0	0	18	0	6
Heavy-Flavor K-factor	0	30	15	0	0	0
Instrumental-ZH-2	0	0	0	0	50	0

TABLE IX: Systematic uncertainties on the contributions for CDF's $H \to W^+W^- \to \ell^\pm\ell'^\mp$ channel. Systematic uncertainties are listed by name, see the original references for a detailed explanation of their meaning and on how they are derived. Systematic uncertainties for H shown in this table are obtained for $m_H = 160$ GeV/c^2. Uncertainties are relative, in percent and are symmetric unless otherwise indicated. The systematic uncertainty called "Normalization" includes effects of the inelastic $p\bar{p}$ cross section, the luminosity monitor acceptance, and the lepton trigger acceptance. It is considered to be entirely correlated with the luminosity uncertainty.

CDF: $H \to WW \to \ell^\pm\ell'^\mp$ Analysis

Contribution	WW	WZ	ZZ	$t\bar{t}$	DY	$W\gamma$	W+jets	H
Trigger	2	2	2	2	3	7	–	3
Lepton ID .	2	1	1	2	2	1	–	2
Acceptance	6	10	10	10	6	10	–	10
$\not\!\!E_T$Modeling	1	1	1	1	20	1	–	1
Conversions	0	0	0	0	0	20	–	0
NNLO Cross Section	10	10	10	15	5	10	–	10
PDF Uncertainty	2	3	3	2	4	2	–	2
Normalization	6	6	6	6	6	6	23	6

TABLE X: Systematic uncertainties on the contributions for DØ's $H \to WW \to \ell^\pm\ell'^\mp$ channel. Systematic uncertainties are listed by name, see the original references for a detailed explanation of their meaning and on how they are derived. Systematic uncertainties shown in this table are obtained for the $m_H = 160$ GeV/c^2 Higgs selection. Uncertainties are relative, in percent and are symmetric unless otherwise indicated.

DØ: $H \to WW \to \ell^\pm\ell'^\mp$ Analysis

Contribution	Diboson	$Z/\gamma^* \to \ell\ell$	$W + jet/\gamma$	$t\bar{t}$	QCD	H
Trigger	5	5	5	5	–	5
Lepton ID .	8–13	8–13	8–13	8–13	–	8–13
Momentum resolution	2–11	2–11	2–11	2–11	–	2–11
Jet Energy Scale	1	1	1	1	–	1
Cross Section	7	6	6	18	–	10
PDF Uncertainty	4	4	4	4	–	4
Normalization	6	6	20	6	30	–

TABLE XI: Systematic uncertainties on the contributions for CDF's $H \to \tau^+\tau^-$ channels. Systematic uncertainties are listed by name, see the original references for a detailed explanation of their meaning and on how they are derived. Uncertainties with provided shape systematics are labeled with "s". Systematic uncertainties for H shown in this table are obtained for $m_H = 115$ GeV/c^2. Uncertainties are relative, in percent and are symmetric unless otherwise indicated. The systematic uncertainty called "Normalization" includes effects of the inelastic $p\bar{p}$ cross section, the luminosity monitor acceptance, and the lepton trigger acceptance. It is considered to be entirely correlated with the luminosity uncertainty.

CDF: $H \to \tau^+\tau^-$ Analysis

Contribution	$Z/\gamma^* \to \tau\tau$	$Z/\gamma^* \to \ell\ell$	$t\bar{t}$	diboson	jet $\to \tau$	W+jet	WH	ZH	VBF	H
Luminosity	6	6	6	6	-	-	6	6	6	6
e, μ Trigger	1	1	1	1	-	-	1	1	1	1
τ Trigger	3	3	3	3	-	-	3	3	3	3
e, μ, τ ID .	3	3	3	3	-	-	3	3	3	3
PDF Uncertainty	1	1	1	1	-	-	1	1	1	1
ISR/FSR	-	-	-	-	-	-	2/0	1/1	3/1	12/1
JES (shape)	16	13	2	10	-	-	3	3	4	14
Cross Section or Norm.	2	2	13	10	-	15	5	5	10	10
MC model	20	10	-	-	-	-	-	-	-	-

TABLE XII: Systematic uncertainties on the contributions for DØ's $WH \to WWW \to \ell'^{\pm}\ell'^{\pm}$ channel. Systematic uncertainties are listed by name, see the original references for a detailed explanation of their meaning and on how they are derived. Systematic uncertainties for WH shown in this table are obtained for $m_H = 160$ GeV/c^2. Uncertainties are relative, in percent and are symmetric unless otherwise indicated.

DØ: $WH \to WWW \to \ell^{\pm}\ell'^{\pm}$ Analysis.

Contribution	WZ/ZZ	Charge flips	QCD	WH
Trigger eff.	5	0	0	5
Lepton ID/Reco. eff	10	0	0	10
Cross Section	7	0	0	6
Normalization	6	0	0	0
Instrumental-ee (ee final state)	0	32	15	0
Instrumental-em ($e\mu$ final state)	0	0	18	0
Instrumental-mm ($\mu\mu$ final state)	0	$^{+290}_{-100}$	32	0

TABLE XIII: Systematic uncertainties on the contributions for DØ's $H \to \gamma\gamma$ channels. Systematic uncertainties are listed by name, see the original references for a detailed explanation of their meaning and on how they are derived. Uncertainties are relative, in percent and are symmetric unless otherwise indicated.

DØ: $H \to \gamma\gamma$ Analysis

Contribution	background	H
Luminosity	6	6
ID efficiency	1	1
Acceptance .	-	2
γ-jet and jet-jet fakes	26	-
electron track-match inefficiency	10–15	-
Cross Section (Z)	4	6
Cross Section (QCD $\gamma\gamma$)	20	-

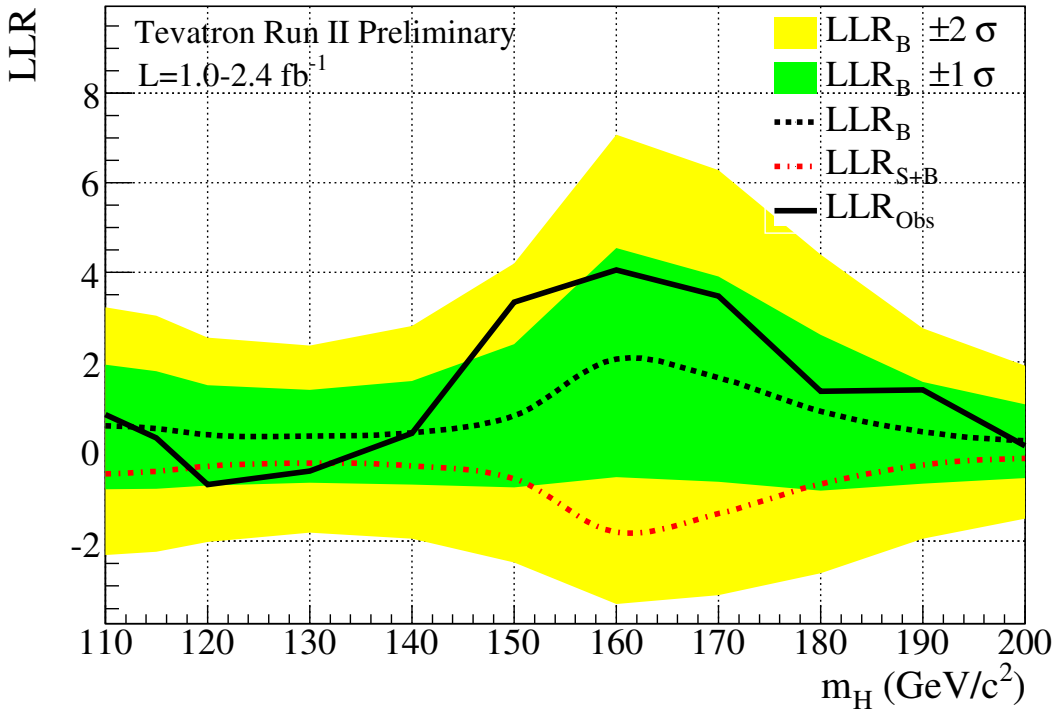

FIG. 1: Distributions of LLR as a function of Higgs mass for the combination of all CDF and DØ analyses.

IV. COMBINED RESULTS

Before extracting the combined limits we study the distributions of the log-likelihood ratio (LLR) for different hypothesis, to check the expected sensitivity across the mass range tested. Figure 1 displays the LLR distributions for the combined analyses as a function of m_H. Included are the results for the background-only hypothesis (LLR_b), the signal and background hypothesis (LLR_{s+b}), and for the data (LLR_{obs}). The shaded bands represent the 1 and 2 standard deviation (σ) departures for LLR_b.

These distributions can be interpreted as follows: The separation between LLR_b and LLR_{s+b} provides a measure of the discriminating power of the search; the size of the 1- and 2-σ LLR_b bands provides an estimate of how sensitive the analysis is to a signal-plus-background-like fluctuation in data, taking account of the systematic uncertainties; the value of LLR_{obs} relative to LLR_{s+b} and LLR_b indicates whether the data distribution appears to be more signal-plus-background-like (i.e. closer to the LLR_{s+b} distribution, which is negative by construction) or background-like; the significance of any departures of LLR_{obs} from LLR_b can be evaluated by the width of the LLR_b bands.

Using the combination procedures outlined in Section III, we extract limits on SM Higgs boson production $\sigma \times B(H \to X)$ in $p\bar{p}$ collisions at $\sqrt{s} = 1.96$ TeV. To facilitate comparisons with the standard model and to accommodate analyses with different degrees of sensitivity, we present our results in terms of the ratio of obtained limits to cross section in the SM, as a function of Higgs boson mass, for test masses for which both experiments have performed dedicated searches in different channels. A value of the combined limit ratio which is less than one would indicate that that particular Higgs boson mass is excluded at the A value < 1 would indicate a Higgs boson mass excluded at

95% C.L. The expected and observed 95% C.L. ratios to the SM cross section for the combined CDF and DØ analyses are shown in Figure 2. The observed and median expected limit ratios are listed for the tested Higgs boson masses in Table XIV, with observed (expected) values of 3.7 (3.3) at $m_H = 115$ GeV/c^2 and 1.1 (1.6) at $m_H = 160$ GeV/c^2.

These results represent about a 40% improvement in expected sensitivity over those obtained on the combinations of results of each single experiment, which yield observed (expected) limits on the SM ratios of 5.0 (4.5) for CDF and 6.4 (5.5) for DØ at $m_H = 115$ GeV/c^2, and of 1.6 (2.6) for CDF and 2.2 (2.4) for DØ at $m_H = 160$ GeV/c^2.

TABLE XIV: Median expected and observed 95% CL cross section ratios for the combined CDF and DØ analyses as a function the Higgs boson mass in GeV/c^2.

	110	115	120	130	140	150	160	170	180	190	200
Expected	3.1	3.3	3.8	4.2	3.5	2.7	1.6	1.8	2.5	3.8	5.1
Observed	2.8	3.7	6.6	5.7	3.5	2.3	1.1	1.3	2.4	2.8	5.2

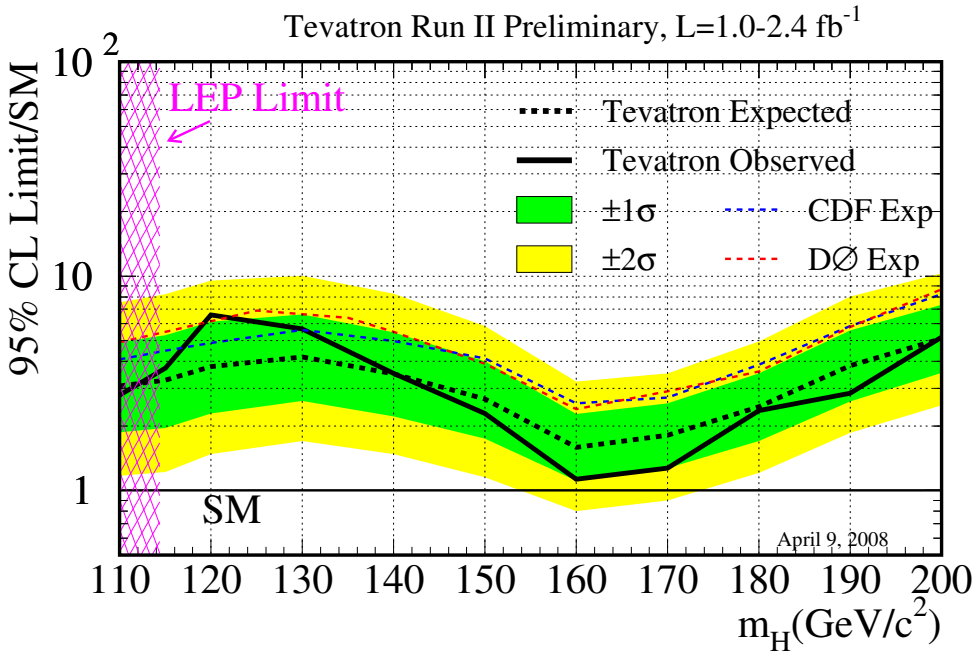

FIG. 2: Observed and expected (median, for the background-only hypothesis) 95% C.L. upper limits on the ratios to the SM cross section, as functions of the Higgs boson test mass, for the combined CDF and DØ analyses. The limits are expressed as a multiple of the SM prediction for test masses for which both experiments have performed dedicated searches in different channels. The WH/ZH with $H \to b\bar{b}$ and the $\tau\tau$ / $\gamma\gamma$ channels are contributing for $m_H \leq 150$ GeV. The $H \to WW$ and $WH \to WWW$ channels are contributing for $m_H \geq 115$ GeV. The points are joined by straight lines for better readability. The bands indicate the 68% and 95% probability regions where the limits can fluctuate, in the absence of signal. Also shown are the expected upper limits obtained for all combined CDF channels, and for all combined DØ channels.

[1] CDF Collaboration, "Combined Upper Limit on Standard Model Higgs Boson Production", CDF Conference Note 8941.

[2] DØ Collaboration, "Combined upper limits on standard model Higgs boson production from the D0 experiment with 1.1-2.4 fb^{-1}" DØ Conference Note 5625.

[3] CDF and DØ Collaborations, "Combined CDF and DØ Upper Limits on Standard Model Higgs-Boson Production", FERMILAB-PUB-07-656-E, arXiv:0712.2383

[4] R. Mommsen for the CDF and DØ Collaborations, XLIIIth Rencontres de Moriond on QCD and High Energy Interactions, 2008, http://moriond.in2p3.fr/QCD/2008/TuesdayAfternoon/Mommsen.pdf

[5] CDF Collaboration, "Search for Higgs Boson Production in Association with W Boson with 1.7 fb^{-1}", CDF Conference Note 8957.

[6] CDF Collaboration, "Search for the Standard Model Higgs Boson in the Missing Et and B-jets Signature", CDF Conference Note 8973.

[7] CDF Collaboration, "Search for ZH in 1 fb-1", CDF Conference Note 8742.

[8] CDF Collaboration, "Search for $H \to WW$ Production Using 1.9 fb^{-1}", CDF Conference Note 8923.

[9] CDF Collaboration, "Search for SM Higgs using tau leptons using 2 fb^{-1}", CDF Conference Note 9179.

[10] DØ Collaboration, "Search for WH Production at $\sqrt{s} = 1.96$ TeV with Neural Networks," DØ Conference Note 5472.

[11] DØ Collaboration, "Search for the standard model Higgs boson in the $HZ \to b\bar{b}\nu\nu$ channel in 2.1 fb-1 of ppbar collisions at $\sqrt{s} = 1.96$ TeV", DØ Conference note 5586.

[12] DØ Collaboration, "A Search for $ZH \to \ell^+\ell^- b\bar{b}$ Production at DØ in $p\bar{p}$ Collisions at $\sqrt{s} = 1.96$ TeV", DØ Conference Note 5482.

[13] DØ Collaboration, "Search for the Higgs boson in $H \to WW^* \to l^+l^-(\ell, \ell' = e\mu)$ decays with 1.7 fb^{-1} at DØ in Run II", DØ Conference Note 5537.

[14] DØ Collaboration, "Search for the Higgs boson in $H \to WW^*$ decays with 1.2 fb^{-1} at DØ in Run IIb", DØ Conference Note 5624.

[15] DØ Collaboration, "Search for associated Higgs boson production $WH \to WWW^* \to \ell^\pm\nu\ell'^\pm\nu' + X$ in $p\bar{p}$ collisions at $\sqrt{s} = 1.96$ TeV", DØ Conference Note 5485.

[16] DØ Collaboration, "Search for a light Higgs boson in $\gamma\gamma$ final state", DØ Conference Note 5601.

[17] T. Sjostrand, L. Lonnblad and S. Mrenna, "PYTHIA 6.2: Physics and manual," arXiv:hep-ph/0108264.

[18] H. L. Lai *et al.*, "Improved Parton Distributions from Global Analysis of Recent Deep Inelastic Scattering and Inclusive Jet Data", Phys. Rev D **55**, 1280 (1997).

[19] S. Catani, D. de Florian, M. Grazzini and P. Nason, "Soft-gluon resummation for Higgs boson production at hadron colliders," JHEP **0307**, 028 (2003) [arXiv:hep-ph/0306211].

[20] K. A. Assamagan *et al.* [Higgs Working Group Collaboration], "The Higgs working group: Summary report 2003," arXiv:hep-ph/0406152.

[21] A. Djouadi, J. Kalinowski and M. Spira, "HDECAY: A program for Higgs boson decays in the standard model and its supersymmetric extension," Comput. Phys. Commun. **108**, 56 (1998) [arXiv:hep-ph/9704448].

[22] M. L. Mangano, M. Moretti, F. Piccinini, R. Pittau and A. D. Polosa, "ALPGEN, a generator for hard multiparton processes in hadronic collisions," JHEP **0307**, 001 (2003) [arXiv:hep-ph/0206293].

[23] S. Frixione and B.R. Webber, JHEP 06, 029 (2002) [arXiv:hep-ph/0204244]

[24] G. Corcella *et al.*, "HERWIG 6: An event generator for hadron emission reactions with interfering gluons (including supersymmetric processes)," JHEP **0101**, 010 (2001) [arXiv:hep-ph/0011363].

[25] A. Pukhov *et al.*, "CompHEP: A package for evaluation of Feynman diagrams and integration over multi-particle phase space. User's manual for version 33," [arXiv:hep-ph/9908288].

[26] J. Campbell and R. K. Ellis, http://mcfm.fnal.gov/.

[27] T. Junk, Nucl. Instrum. Meth. A434, p. 435-443, 1999, A.L. Read, "Modified frequentist analysis of search results (the CL_s method)", in F. James, L. Lyons and Y. Perrin (eds.), *Workshop on Confidence Limits*, CERN, Yellow Report 2000-005, available through `cdsweb.cern.ch`.